

PAPER

View Article Online
View Journal | View Issue

Site-selective methylene C–H oxidation of an alkyl diamine enabled by supramolecular recognition using a bioinspired manganese catalyst†

Arnau Vicens,^a Laia Vicens,^a ^a Giorgio Olivo,^a ^{*b} Osvaldo Lanzalunga,^b ^b Stefano Di Stefano ^b and Miquel Costas ^{*a}

Received 16th December 2022, Accepted 6th January 2023

DOI: 10.1039/d2fd00177b

Site-selective oxidation of aliphatic C–H bonds is a powerful synthetic tool because it enables rapid build-up of product complexity and diversity from simple precursors. Besides the poor reactivity of alkyl C–H bonds, the main challenge in this reaction consists in differentiating between the multiple similar sites present in most organic molecules. Herein, a manganese oxidation catalyst equipped with two 18-benzo-6-crown ether receptors has been employed in the oxidation of the long chain tetradecane-1,14-diamine. ¹H-NMR studies evidence simultaneous binding of the two protonated amine moieties to the crown ether receptors. This recognition has been used to pursue site-selective oxidation of a methylenic site, using hydrogen peroxide as oxidant in the presence of carboxylic acids as co-ligands. Excellent site-selectivity towards the central methylenic sites (C6 and C7) is observed, overcoming selectivity parameters derived from polar deactivation by simple amine protonation and selectivity observed in the oxidation of related monoprotonated amines.

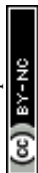
Introduction

Selective functionalization of alkyl C–H bonds is one of the most challenging reactions in organic chemistry because of the poorly reactive character of these bonds.¹ Moreover, organic molecules commonly have many methylenic site with similar electronic and steric properties, which make them difficult to be differentiated. Governing site-selectivity is especially challenging in the oxidation of long aliphatic chains, where methylenic site are nearly equivalent from

^aInstitut de Química Computacional i Catàlisi (IQCC) and Departament de Química, Universitat de Girona, Campus de Montilivi, 17071 Girona, Spain. E-mail: miquel.costas@udg.edu

^bDipartimento di Chimica and Istituto CNR di Metodologie Chimiche (IMC-CNR), Sezione Meccanismi di Reazione, Sapienza Università di Roma, P.le A. Moro 5, I-00185 Rome, Italy. E-mail: giorgio.olivo@uniroma1.it

† Electronic supplementary information (ESI) available. See <https://doi.org/10.1039/d2fd00177b>



a reactivity perspective. In these cases, C–H functionalization reactions usually proceed to yield a statistical distribution of products. However, site-selectivity has been pursued by using bulky catalysts that disfavor oxidation of internal sites that are sterically more demanding,² or *via* intramolecular reactions governed by directing groups.³

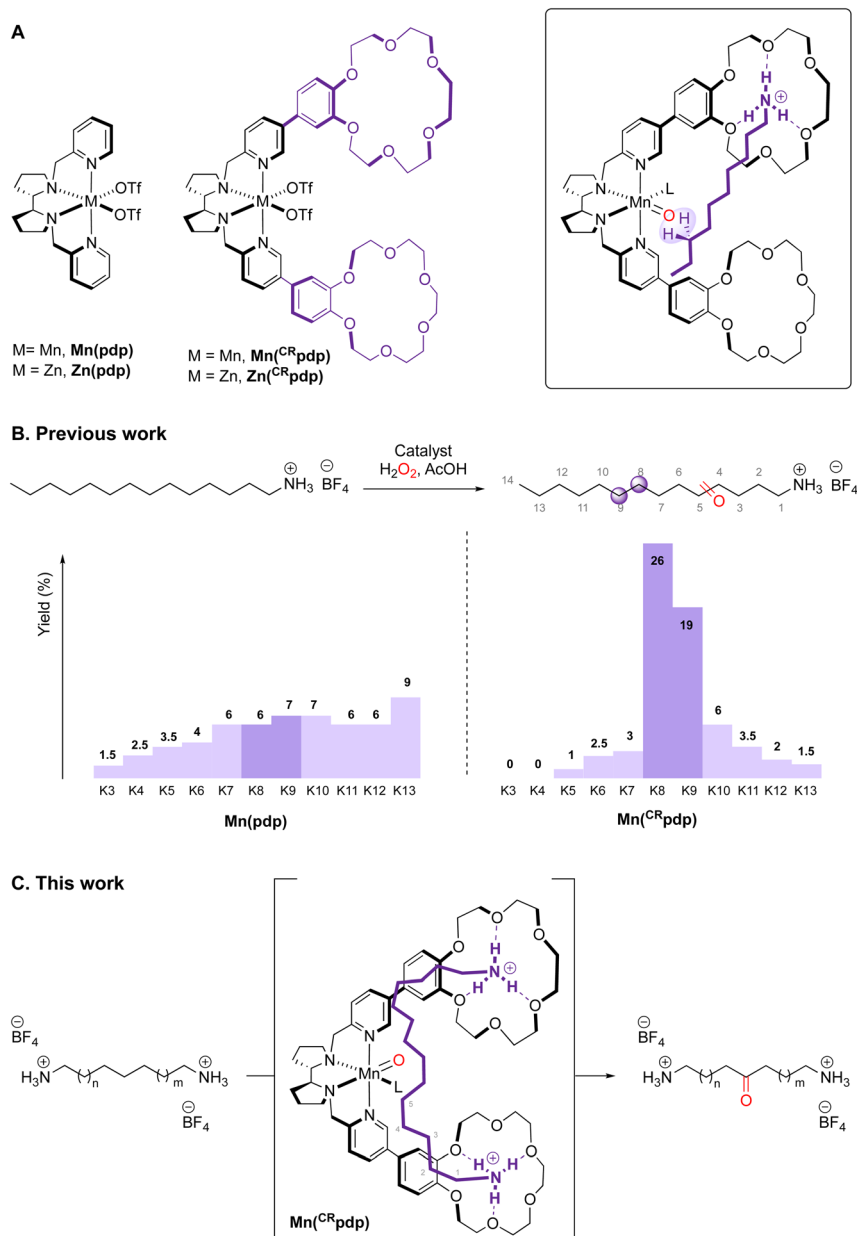


Fig. 1 (A) Catalyst with and without 18-benzocrown-6-ether receptors and their interaction with protonated amines. (B) Previous work on the oxidation of linear protonated amines. (C) This work.



An appealing strategy to pursue site-selectivity is the use of weak interactions, akin to those operating in enzymatic sites.⁴ Supramolecular interactions may be used to govern the access and/or positioning of the substrate with respect to the catalytic site, promoting the reactivity of specific well-oriented positions of the substrate.⁵ One strategy consists in using supramolecular hosts that embed the catalyst and only permit access to substrate sites readily accessible or with specific 3D structure.⁶ Alternatively, catalysts may be equipped with a receptor that recognizes specific functional groups in the substrate leading to an exposure of specific sites to the reactive center. A critical aspect of this strategy is the use of weak interactions that ensures reversible binding of the substrate to the catalyst, enabling catalyst turnover and reducing product inhibition. Pioneering examples of the use of supramolecular receptors to govern site-selectivity in C–H oxidation have been described by Breslow,⁷ and more recently by Crabtree and Brudvig,⁸ Bach⁹ and Tiefenbacher.¹⁰

Recently, we reported a Mn catalyst based on a N₂Py₂ ligand in which 18-benzocrown-6-ether receptors ([Mn(CF₃SO₃)₂(^{CR}pdp)], **Mn**^{CR}**pdp**)¹¹ that have high affinity towards protonated primary amines were attached (Fig. 1A). A notable increase in selectivity towards C8 and C9 methylenic sites is achieved as the protonated amine is recognized by the crown ether (Fig. 1B).¹²

Building on these precedents, the aim of this work is to explore site-selective C–H oxidations on the aliphatic chain of a protonated diamine that can bind simultaneously to the two crown ether receptors of a single catalyst. It was envisioned that, in such a case, the reduction of the degrees of freedom of the substrate upon binding to the catalyst will translate into an enhanced site-selectivity. Towards this end, the binding of the long-chain 1,14-tetradecanedia-monium tetrafluoroborate (**S1**), selected as substrate, to **Zn**(^{CR}**pdp**), the Zn analogue of the manganese catalyst **Mn**(^{CR}**pdp**), was explored by NMR. Oxidation of **S1** with **Mn**(^{CR}**pdp**), H₂O₂ and a carboxylic acid was then studied. Compared with the previously described oxidation of monoamine substrates,¹¹ the current reactions evidence substantially improved site-selectivities. Comparison with values obtained with a simple **Mn**(**pdp**) catalyst¹³ permits one to distinguish the contributions to selectivity derived from supramolecular recognition from those due to polar effects resulting from the repulsion between the ammonium groups and the electrophilic catalyst.

Results and discussion

The recently described catalysts **Mn**(^{CR}**pdp**)¹¹ and its Zn analogue **Zn**(^{CR}**pdp**)¹⁴ were employed in the study. Catalytic oxidation of **S1** was performed using **Mn**(^{CR}**pdp**) as the catalyst. In addition, control experiments were done with **Mn**(**pdp**), the complex that has the same structure as **Mn**(^{CR}**pdp**) but lacks the supramolecular 18-benzocrown-6-ether receptors.

¹H-NMR studies of the binding of **S1** to **Zn**(^{CR}**pdp**)

The diamagnetic Zn complex **Zn**(^{CR}**pdp**) shares the same topology and first coordination sphere of the metal as in **Mn**(^{CR}**pdp**), and, therefore, it is envisioned as a suitable probe to characterize the substrate–catalyst binding by ¹H-NMR.¹³

Titration of 1.0 mM **Zn**(^{CR}**pdp**) with **S1** was followed by ¹H-NMR (CD₃CN, 25 °C). Focusing on the region between 3.3–4.6 ppm (Fig. 2A), a downfield shift of the



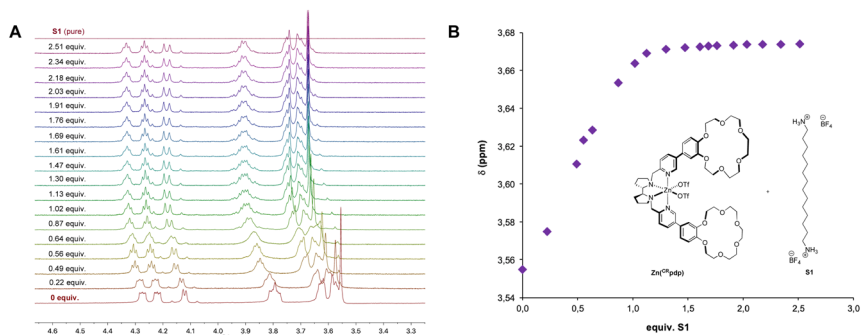


Fig. 2 Binding of **S1** to $\text{Zn}^{\text{CR}}\text{pdp}$ (1 mM) in CD_3CN at 25 °C. (A) Enlargement of the region between 3.3 and 4.6 ppm, corresponding to the crown ether signals. (B) Titration curve.

crown ether signals was observed upon addition of **S1**, suggesting that the protonated diamine moieties interact with the crown ether. Moreover, the observed saturation profile, which reaches a plateau after addition of 1.0–1.2 molar equivalents of **S1**, indicates a 1 : 1 host–guest stoichiometry ($K_{\text{ass}} > 10^3 \text{ M}^{-1}$, Fig. 2B).

Two binding modalities can be considered for a 1 : 1 stoichiometry between the substrate and the catalyst. The first possibility is that a diamine molecule may

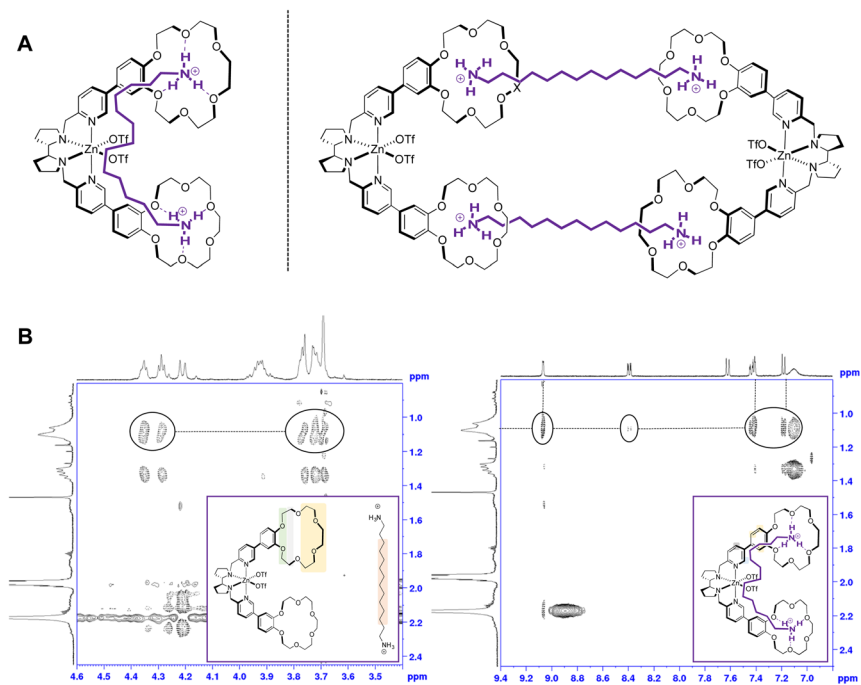


Fig. 3 (A) Possible 1 : 1 stoichiometries for $\text{Zn}^{\text{CR}}\text{pdp}:\text{S1}$ binding. (B) NOESY of the 1 : 1 mixture of $\text{Zn}^{\text{CR}}\text{pdp}:\text{S1}$. (Left): enlargement of the aliphatic region of the crown ether catalyst (3.5–4.5 ppm) vs. **S1** signals (0.8–2.5 ppm). (Right): enlargement of the aromatic region of the catalyst (7.0–9.4 ppm) vs. **S1** signals (0.8–2.5 ppm).



be bound to a single molecule of catalyst, each end of the substrate interacting with one of the two crown ether receptors of the same catalyst molecule (Fig. 3A, left). A second option consistent with the stoichiometry is that each diamine binds to two crown ether moieties that belong to different catalyst molecules, which would result in the formation of cyclo-oligomeric species, the dimer being the simplest possibility (Fig. 3A, right).

To understand how the substrate binds to the catalyst, two-dimensional NMR NOESY experiments were carried out with a 1 : 1 mixture of $\text{Zn}(\text{CR}^{\text{pdp}})\text{:S1}$ (Fig. 3B). First, in the aliphatic region of the crown ether catalyst, an intermolecular NOESY correlation between the signals of the crown ether (3.5–4.5 ppm) and those of the substrate was observed (Fig. 3B, left), which implies proximity between the diamine and the crown ether moieties of the complex, in accordance with the adduct geometry observed with monoamines.¹⁴ Second and more interestingly, a clear NOESY correlation between the aliphatic signals of the substrate and the α -protons of the pyridines of the ligand was observed, as well as with the protons of the phenyl ring of the benzocrown. A small correlation was also observed with the γ -proton of the pyridine rings. These correlations are only consistent with the 1 : 1 model depicted in Fig. 3A (left), in which the protonated diamine is located close to the aromatic parts of $\text{Zn}(\text{CR}^{\text{pdp}})$, and are incompatible with the 2 : 2 adduct on the right. The 1 : 1 stoichiometry, which therefore prevails on all other $n : n$ ones ($n > 1$), is consistent with the desired recognition-driven site-selective oxidation.

A control experiment with $\text{Zn}(\text{pdp})$, devoid of the crown ether, was also performed following an analogous procedure. In this case, no shift in either the signals of the catalyst nor the signals of **S1** was detected, suggesting the absence of any interaction. A NOESY experiment on the 1 : 1 mixture of $\text{Zn}(\text{pdp})\text{:S1}$ did not show any intermolecular correlation, which confirms the expected lack of binding between the substrate and the complex.

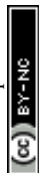
Catalytic oxidation of **S1**

Once the desired binding geometry between **S1** and the supramolecular catalyst was confirmed, oxidation of the substrate was investigated. Catalytic oxidations were performed adopting the following standard conditions: 1 mol% of catalyst, 1 equiv. of **S1** (0.1 M), 10 equiv. of H_2O_2 delivered by a syringe pump over 30 minutes, and 22 equiv. of AcOH at 0 °C.¹¹ Conversions and yields were determined by $^1\text{H-NMR}$ (Fig. 4A).

Oxidation of the different methylenic sites of **S1** produced a mixture of isomeric alcohol (OH) and ketone (K) products differing in the position of the oxygenated function (*i.e.*, K2 refers to the ketone derived from oxidation of the C2 site, *etc.*). Site-selectivity (the distribution of the isomeric oxygenated products) was analyzed by GC after derivatization of the products by the preparation of the corresponding dipivalamides (Fig. 4B). The oxidation site was assigned by analyzing the fragmentation of the ketone products in the EI-MS spectra (Fig. 4C).¹¹

The results obtained are shown in Table 1. For each reaction, the analysis of site-selectivity was repeated after Jones oxidation of the reaction mixture to convert all the alcohols into ketones (Table 1, footnote *d*).

When using $\text{Mn}(\text{pdp})$ as the catalyst, a 26% combined yield of ketones and 5% of alcohols was obtained, with a selectivity for the central C6 and C7 sites of 62%.



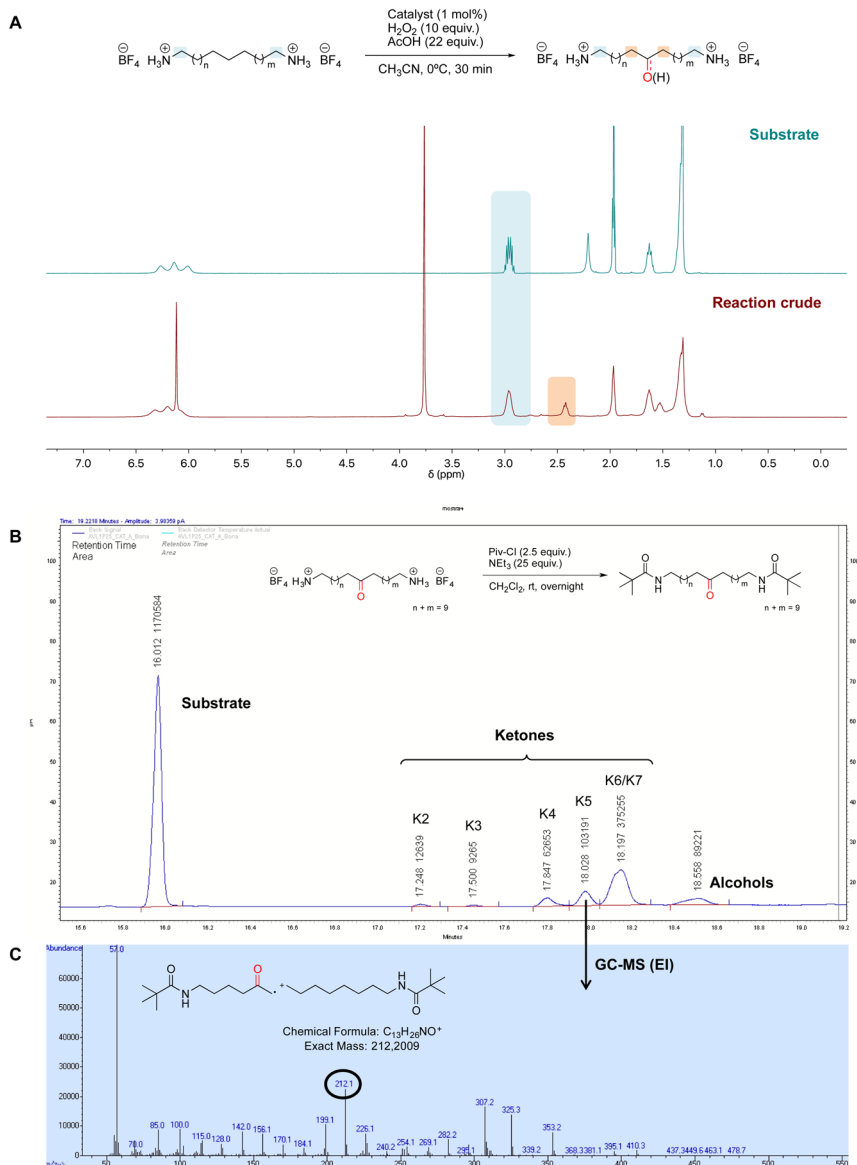


Fig. 4 Experimental details for oxidation of **S1**. (A) NMR spectrum of **S1** before (top) and after the oxidation (bottom; sharp peaks at 3.7 and 6.1 ppm are due to 1,3,5-trimethoxybenzene internal standard). (B) GC chromatogram of the oxidation of **S1** with the **Mn(pdp)** catalyst analyzed after derivatization of products. (C) GC-MS (EI) of the peak at 18.0 min, showing the fragmentation of product **K5** as a typical example of fragmentation.

Significant amounts of **K4** and **K5** were also obtained. The origin of this selectivity is likely due to the polar deactivation exerted by the protonated amine moieties, which decreases as the methylenic site moves away from the NH₃⁺. In contrast, when the supramolecular catalyst **Mn^{CR}pdp** was used, the total yield of oxidation products was slightly increased, the mass balance of the reaction substantially improved (35% combined yield/38% substrate conversion) and, most



Table 1 Oxidation of **S1** with different catalysts

Catalyst [x mol%]	Conv. ^a (%)	Yield K ^a (%)	Yield OH ^b (%)	K2 ^c	K3 ^c	K4 ^c	K5 ^c	K6 + K7 ^c
—	4	—	—	—	—	—	—	—
Mn(pdp) [1 mol%]	45	26	5	2	2	11	18	67
				6 ^d	1 ^d	14 ^d	17 ^d	62 ^d
Mn(CR<pdp)< b=""> [1 mol%]</pdp)<>	38	25	10	0	2	7	6	84
				2 ^d	3 ^d	5 ^d	10 ^d	81^d
Mn(CR<pdp)< b=""> [3 mol%]</pdp)<>	55	43	7	0	1	6	7	86
				0 ^d	2 ^d	2 ^d	8 ^d	88^d

^a Conversions and yields determined by ¹H-NMR using 1,3,5-trimethoxybenzene as the internal standard. ^b Estimated by GC. ^c Normalized site-selectivity (%) determined by GC after derivatization. ^d Values obtained after oxidation of the mixture with Jones reagent.

remarkably, the selectivity towards K6 + K7 increased up to 81%. This means that supramolecular recognition plays an important role as the selectivity increases from 62% to 81% compared to the reaction in the absence of supramolecular recognition. With higher catalyst loading (3 mol%), the oxidation yield and the selectivity for C6 and C7 sites increased up to 43% and, remarkably, 88%, respectively. A notable finding concerns the relative selectivity for C4 and C5 oxidation. In the absence of the recognition, the two positions are nearly equally reactive. In contrast, in the presence of the crown ether moieties, oxidation at C4 is substantially prevented, since such a position is presumably placed far away from the reactive metal-oxo in the catalyst–substrate complex.

Effect of carboxylic acid co-catalyst

Carboxylic acids are known to be crucial co-ligands in oxidation reactions, and different examples in the literature showed that modulation of their structure may affect the selectivity of the oxidation reactions.^{2c} The active species responsible for the C–H oxidation with this specific type of catalyst is presumably a Mn^V(O)(-carboxylate) intermediate,¹⁵ and therefore the nature of the carboxylate ligand impacts on the structure of the C–H cleaving species. In fact, use of different carboxylic acid co-ligands allowed fine-tuning of site- and enantio-selectivity of C–H oxidation reactions catalysed by the same Mn catalyst. Along this line, we explored replacement of acetic acid with other more structured acids in order to pursue an improvement of the selectivity for the central C6 and C7 sites (Table 2).¹⁶ All these experiments were performed with 1 mol% of catalyst **Mn(CR.**

As shown in Table 2, all the tested carboxylic acids were effective co-catalysts, with the exception of 1-adamantane carboxylic acid (entry 2), Phth-Gly-OH (entry 5) and dichloroacetic acid (entry 8) that delivered no oxidation products. Cyclopropyl carboxylic acid (entry 6) and 3,3-dimethylbutyric carboxylic acid (entry 7) gave similar selectivity to acetic acid (entry 1), while 2-ethylbutyric carboxylic acid led to slightly lower values (entry 3). More interestingly, a series of bulky

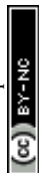
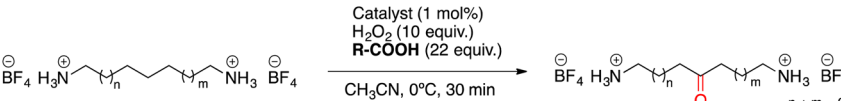
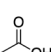
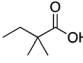
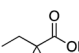


Table 3 Oxidation of **S1** using different catalysts and different carboxylic acids

$ \begin{array}{c} \text{Catalyst (1 mol\%)} \\ \text{H}_2\text{O}_2 \text{ (10 equiv.)} \\ \text{R-COOH (22 equiv.)} \\ \text{CH}_3\text{CN, 0}^\circ\text{C, 30 min} \end{array} $									
$ \text{BF}_4^- \text{H}_3\text{N}^+ \text{---} (\text{CH}_2)_n \text{---} (\text{CH}_2)_m \text{---} \text{NH}_3^+ \text{BF}_4^- \longrightarrow \text{BF}_4^- \text{H}_3\text{N}^+ \text{---} (\text{CH}_2)_n \text{---} \text{C(=O)} \text{---} (\text{CH}_2)_m \text{---} \text{NH}_3^+ \text{BF}_4^- $									
R-COOH	Catalyst	Conv. ^a (%)	Yield K ^a (%)	Yield OH ^b (%)	K2 ^c	K3 ^c	K4 ^c	K5 ^c	K6 + K7 ^c
	Mn(pdp)	45	26	5	2	2	11	18	67
	Mn(CR^{CR}pdp)	38	25	10	0	2	7	6	84
	Mn(pdp)	62	34	0	2	0	12	3	82
	Mn(CR^{CR}pdp)	35	24	4	0	1	6	2	91
	Mn(pdp)	37	27	4	0	0	11	12	77
	Mn(CR^{CR}pdp)	51	42	4	0	3	5	1	91
	Mn(pdp)	40	15	6	0	0	15	6	79
	Mn(CR^{CR}pdp)	55	38	3	0	2	5	1	92

^a Conversions and yields determined by ¹H-NMR using 1,3,5-trimethoxybenzene as the internal standard. ^b Estimated by GC. ^c Normalized site-selectivity (%) determined by GC after derivatization.

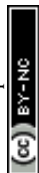
porphyrin and 2,6-dichloro-pyridine *N*-oxide oxidant. In both reports, up to >90% selectivity for the oxidation of the two central methylenic sites was obtained in the best cases, which compares well with the present findings. Such selectivities are higher than those previously obtained with singly bound alkyl chain monoamines (up to 81% selectivity for the two favoured methylenes).^{10,11} Under oxidation conditions, catalyst **Mn(CR^{CR}pdp)** is expected to be almost fully saturated (>98%) with both diammonium **S1** and monoammonium guests. Hence, the increased selectivity observed with diammonium **S1** can be ascribed to an improved pre-organization of the catalyst–substrate adduct that arises from the higher rigidity associated with the two-point binding of **S1**.

Conclusion

In summary, we have demonstrated the capability of a bioinspired manganese catalyst bearing two benzocrown ether receptors for binding a diprotonated diamine. The binding mainly occurs in a 1 : 1 stoichiometry, with each protonated amine of the substrate being recognized by one of the two crown ether receptors of the catalyst, resulting in a well-defined orientation of the substrate towards the metal center. In the catalytic oxidation of a diammonium substrate, such binding allows an increase of selectivity for the central C6 and C7 positions up to 92% using bulky carboxylic acids as co-ligands.

Conflicts of interest

There are no conflicts to declare.



Acknowledgements

This work was supported by the Spanish Ministry of Science, Innovation, and Universities (PID2021-129036NB-I00 to M. C. and PhD grant FPU16/04231 to L.V.), and Generalitat de Catalunya (ICREA Academia Award to M.C.). G.O. acknowledges project S-ReCHOx from SCI and Elsevier for funding. We acknowledge STR of UdG for experimental support.

References

- 1 T. Newhouse and P. S. Baran, *Angew. Chem., Int. Ed.*, 2011, **50**, 3362.
- 2 (a) M. C. White and J. Zhao, *J. Am. Chem. Soc.*, 2018, **140**, 13988; (b) W. Sun and Q. Sun, *Acc. Chem. Res.*, 2019, **52**, 2370; (c) L. Vicens, G. Olivo and M. Costas, *ACS Catal.*, 2020, **10**, 8611.
- 3 (a) T. Brückl, R. D. Baxter, Y. Ishihara and P. S. Baran, *Acc. Chem. Res.*, 2012, **45**, 826; (b) S. Bhadra and H. Yamamoto, *Chem. Rev.*, 2018, **118**, 3391.
- 4 (a) J. C. Lewis, P. S. Coelho and F. H. Arnold, *Chem. Soc. Rev.*, 2011, **40**, 2003; (b) R. Fasan, *ACS Catal.*, 2012, **2**, 647; (c) S. Jena, J. Dutta, K. D. Tulsiyan, A. K. Sahu, S. S. Choudhury and H. S. Biswal, *Chem. Soc. Rev.*, 2022, **51**, 4261.
- 5 (a) P. Dydio and J. N. H. Reek, *Chem. Sci.*, 2014, **5**, 2135; (b) H. J. Davis and R. J. Phipps, *Chem. Sci.*, 2017, **8**, 864; (c) D. Vidal, G. Olivo and M. Costas, *Chem.–Eur. J.*, 2018, **24**, 5042; (d) G. Olivo, G. Capocasa, D. Del Giudice, O. Lanzalunga and S. Di Stefano, *Chem. Soc. Rev.*, 2021, **50**, 7681; (e) S. Pachisia and R. Gupta, *Dalton Trans.*, 2021, **50**, 14951; (f) Y. Jiao, X.-Y. Chen and J. F. Stoddart, *Chem*, 2022, **8**, 414.
- 6 (a) M. Guitet, P. Zhang, F. Marcelo, C. Tugny, J. Jiménez-Barbero, O. Buriez, C. Amatore, V. Mouriès-Mansuy, J.-P. Goddard, L. Fensterbank, Y. Zhang, S. Roland, M. Ménand and M. Sollogoub, *Angew. Chem., Int. Ed.*, 2013, **52**, 7213; (b) C. García-Simón, R. Gramage-Doria, S. Raoufmoghaddam, T. Parella, M. Costas, X. Ribas and J. N. H. Reek, *J. Am. Chem. Soc.*, 2015, **137**, 2680; (c) T. A. Bender, R. G. Bergman, K. N. Raymond and F. D. Toste, *J. Am. Chem. Soc.*, 2019, **141**, 11806.
- 7 (a) R. Breslow, Y. Huang, X. Zhang and J. Yang, *Proc. Natl. Acad. Sci. U. S. A.*, 1997, **94**, 11156; (b) R. Breslow, X. Zhang and Y. Huang, *J. Am. Chem. Soc.*, 1997, **119**, 4535; (c) J. Yang, B. Gabriele, S. Belvedere, Y. Huang and R. Breslow, *J. Org. Chem.*, 2002, **67**, 5057.
- 8 S. Das, C. D. Incarvito, R. H. Crabtree and G. W. Brudvig, *Science*, 2006, **312**, 1941.
- 9 (a) F. Burg, M. Gicquel, S. Breitenlechner, A. Pöthig and T. Bach, *Angew. Chem., Int. Ed.*, 2018, **57**, 2953; (b) F. Burg, S. Breitenlechner, C. Jandl and T. Bach, *Chem. Sci.*, 2020, **11**, 2121; (c) F. Burg, C. Buchelt, N. M. Kreienborg, C. Merten and T. Bach, *Org. Lett.*, 2021, **23**, 1829.
- 10 (a) M. Knezevic, M. Heilmann, G. M. Piccini and K. Tiefenbacher, *Angew. Chem., Int. Ed.*, 2020, **59**, 12387; (b) M. Knezevic and K. Tiefenbacher, *Chem.–Eur. J.*, 2022, e202203480.
- 11 (a) G. Olivo, G. Farinelli, A. Barbieri, O. Lanzalunga, S. Di Stefano and M. Costas, *Angew. Chem., Int. Ed.*, 2017, **56**, 16347; (b) G. Olivo, G. Capocasa, O. Lanzalunga, S. Di Stefano and M. Costas, *Chem. Commun.*, 2019, **55**, 917.



- 12 S. Di Stefano, G. Capocasa and L. Mandolini, *Eur. J. Org. Chem.*, 2020, **2020**, 3340.
- 13 R. V. Ottenbacher, D. G. Samsonenko, E. P. Talsi and K. P. Bryliakov, *Org. Lett.*, 2012, **14**, 4310.
- 14 (a) G. Olivo, G. Capocasa, B. Ticconi, O. Lanzalunga, S. Di Stefano and M. Costas, *Angew. Chem., Int. Ed.*, 2020, **59**, 12703; (b) L. Vicens, G. Olivo and M. Costas, *Angew. Chem., Int. Ed.*, 2022, **61**, e202114932.
- 15 (a) R. V. Ottenbacher, E. P. Talsi and K. P. Bryliakov, *ACS Catal.*, 2015, **5**, 39; (b) X.-X. Li, M. Guo, B. Qiu, K.-B. Cho, W. Sun and W. Nam, *Inorg. Chem.*, 2019, **58**, 14842.
- 16 (a) M. Milan, M. Bietti and M. Costas, *ACS Cent. Sci.*, 2017, **3**, 196; (b) E. P. Talsi, D. G. Samsonenko, R. V Ottenbacher and K. P. Bryliakov, *ChemCatChem*, 2017, **9**, 4580–4586; (c) B. Qiu, D. Xu, Q. Sun, C. Miao, Y.-M. Lee, X.-X. Li, W. Nam and W. Sun, *ACS Catal.*, 2018, **8**, 2479–2487; (d) M. Galeotti, L. Vicens, M. Salamone, M. Costas and M. Bietti, *J. Am. Chem. Soc.*, 2022, **144**, 7391.
- 17 R. Breslow, R. Rajagopalan and J. Schwarz, *J. Am. Chem. Soc.*, 1981, **103**, 2905.
- 18 S. Teramae, A. Kito, T. Shingaki, Y. Hamaguchi, Y. Yano, T. Nakayama, Y. Kobayashi, N. Kato, N. Umezawa, Y. Hisamatsu, T. Nagano and T. Higuchi, *Chem. Commun.*, 2019, **55**, 8378.

